

In Vivo Persistence of Codominant Human CD8⁺ T Cell Clonotypes Is Not Limited by Replicative Senescence or Functional Alteration¹

Laurent Derré,^{2*} Marc Bruyninx,^{2*†} Petra Baumgaertner,^{*} Estelle Devevre,^{*} Patricia Corthesy,[†] Cédric Touvrey,^{*} Yolanda D. Mahnke,[‡] Hanspeter Pircher,[§] Verena Voelter,^{||} Pedro Romero,^{*} Daniel E. Speiser,^{2*} and Nathalie Rufer^{2,3†}

T cell responses to viral epitopes are often composed of a small number of codominant clonotypes. In this study, we show that tumor Ag-specific T cells can behave similarly. In a melanoma patient with a long lasting HLA-A2/NY-ESO-1-specific T cell response, reaching 10% of circulating CD8 T cells, we identified nine codominant clonotypes characterized by individual TCRs. These clonotypes made up almost the entire pool of highly differentiated effector cells, but only a fraction of the small pool of less differentiated “memory” cells, suggesting that the latter serve to maintain effector cells. The different clonotypes displayed full effector function and expressed TCRs with similar functional avidity. Nevertheless, some clonotypes increased, whereas others declined in numbers over the observation period of 6 years. One clonotype disappeared from circulating blood, but without preceding critical telomere shortening. In turn, clonotypes with increasing frequency had accelerated telomere shortening, correlating with strong in vivo proliferation. Interestingly, the final prevalence of the different T cell clonotypes in circulation was anticipated in a metastatic lymph node withdrawn 2 years earlier, suggesting in vivo clonotype selection driven by metastases. Together, these data provide novel insight in long term in vivo persistence of T cell clonotypes associated with continued cell turnover but not replicative senescence or functional alteration. *The Journal of Immunology*, 2007, 179: 2368–2379.

Cytolytic CD8⁺ T lymphocytes play an important role in adaptive immunity and are responsible for specific recognition and elimination of infected or transformed cells. Recognition of such cells relies on the specific interaction of clonally distributed TCRs on effector lymphocytes with Ag-derived peptides bound to self-MHC molecules on infected or malignant cells (1). The introduction of fluorescent multimers of MHC/peptide that bind stably to specific TCR on the surface of T cells has enabled detailed TCR repertoire analysis of Ag-specific T cells isolated ex vivo (2, 3).

The CD8⁺ T cell responses to primary virus infections are characterized by large expansions of activated T cell clones bearing particular TCRs (4). In humans, highly restricted TCR usage has been described in several viral systems, including influenza (5, 6),

EBV (7, 8), CMV (9), and HIV-1 (10–12). Thus, the limited TCR diversity seems to be a conserved feature of CD8⁺ T cell responses to viral infection. Our group recently identified a naturally primed T cell clone that dominated the human CD8⁺ T cell response to the Melan-A/MART-1 tumor Ag (13). Taken together, our data and those reported by others (reviewed in Ref. 14) indicate that similar to T cell responses against immunodominant viral Ags, selection and amplification of tumor-specific T cell clones occurs in cancer patients.

Long-term persistence of clonally restricted CD8⁺ T cell expansions has been observed in chronic viral infections such as EBV (15, 16), HSV (17), or HIV (11, 18, 19). In line with these studies, individual T cell clonotypes expressing high avidity TCRs to cognate tumor Ag were detected in melanoma patients with favorable disease outcome (20), as well as in a patient vaccinated repeatedly with Melan-A_{26–35} peptide mixed with IFA and CpG 7909 over extended periods of time (13). Despite major progress in the analysis of Ag-specific T cells, however, in vivo TCR repertoire evolutions in response to chronic antigenic exposure, e.g., in viral infection (EBV, HIV) or in the tumor-bearing state, remain largely unexplored. Furthermore, most of these studies provide limited information concerning the factors controlling turnover and persistence of particular T cell clonotypes. These questions are fundamental to our understanding of protective immunity and have important implications for vaccine design and development.

In the present study, we explored a natural tumor-specific immune response against the cancer testis Ag NY-ESO-1, subsequently boosted by peptide vaccination in a melanoma patient. To study and define the molecular evolution of epitope-specific CD8⁺ T lymphocytes, we used a novel ex vivo molecular-based approach at the single cell level (13). We identified nine distinct and codominant T cell clonotypes bearing BV1, BV8, or BV13 TCRs. Over a period of several years, we observed changes in frequencies of

*Division of Clinical Onco-Immunology, Ludwig Institute for Cancer Research, University Hospital of Lausanne, Lausanne, Switzerland; †Swiss Institute for Experimental Cancer Research, Epalinges, Switzerland; ‡Vaccine Research Center, National Institute of Allergy and Infectious Diseases, National Institutes of Health, Bethesda, MD 20892; §Institute for Medical Microbiology and Hygiene, Department of Immunology, University of Freiburg, Freiburg, Germany; and ||Multidisciplinary Oncology Center, Centre Hospitalier Universitaire Vaudois (CHUV), Lausanne, Switzerland

Received for publication March 26, 2007. Accepted for publication May 30, 2007.

The costs of publication of this article were defrayed in part by the payment of page charges. This article must therefore be hereby marked *advertisement* in accordance with 18 U.S.C. Section 1734 solely to indicate this fact.

¹ This study was sponsored and supported by the Swiss National Center of Competence in Research (NCCR) Molecular Oncology, the Ludwig Institute for Cancer Research, the Cancer Research Institute, NY, the Swiss Cancer League/Oncosuisse Grant 01323-02-2003, and the Swiss National Science Foundation Grants 3200B0-107693 and 3100A0-105929.

² L.D., M.B., D.S., and N.R. contributed equally to this work.

³ Address correspondence and reprint requests to Dr. Nathalie Rufer, Swiss Institute for Experimental Cancer Research, 155 ch. des Boveresses, Epalinges, Switzerland. E-mail address: Nathalie.Rufer@isrec.ch

clonotypes with an expansion of BV13 T cells, and decrease and even disappearance of BV8 subpopulations. Clonotypic fluctuations were concomitant to vaccination with NY-ESO-1 analog peptide. We quantified differentiation, proliferative potential, and ability to produce effector mediators and cytokines. Because our analysis was performed on individual T cell clonotypes, it provides, for the first time, a detailed insight in factors associated with persistence and survival of tumor-specific T cell subpopulations.

Materials and Methods

Clinical history

Patient LAU 50, HLA-A*0201 positive, was diagnosed at the age of 62 years with primary skin melanoma of the right leg in January 1992. Breslow tumor thickness was 4.3 mm. In the following year he developed multiple skin metastases in the right leg and was treated with isolated limb perfusion with melphalan, TNF- α , and IFN- γ . Five inguinal lymph nodes were removed and found tumor free. Two years later he developed a single inguinal lymph node metastasis, and inguinoaxillary lymph node dissection revealed that 13/14 nodes were tumor free. Eight years later (in November 2003) he had a contralateral metastasis (i.e., left inguinal), which was removed in January 2004 (–3 mo before the start of vaccination). Similar to the previous lesions, this metastasis expressed multiple tumor Ags, i.e., Melan-A, gp100, Tyr, Mage-1, Mage-3, Mage-10, Lage-1, NY-ESO-1, SSX-2, and SSX-4. Starting April 2004 (D0), the patient was enrolled in the Ludwig Institute vaccination trial LUD 01-003 (21) and received 12 monthly s.c. vaccines (until +13 mo) composed of 3×500 mg of peptide (NY-ESO-1_{157–165} SLLMWITQA C165A analog, Mage-A10_{254–262} GLYDGM EHL and Melan-A_{26–35} ELAGIGILTV A27L analog), emulsified in 1 ml of Montanide ISA-51, prepared altogether in one syringe as a stable emulsion (2-ml injection volume). Peptides were provided by ClinAlfa, MerckBiosciences, Läufelfingen, Switzerland, and adjuvant IFA; Montanide ISA-51 was provided by Seppic. Increased frequencies of Mage-A10 Ag-specific CD8⁺ T lymphocytes were observed in patient LAU 50 upon vaccination, with values reaching up 0.16% of CD8⁺ T cells (21). Future studies involve the molecular characterization of such tumor-specific T cells. In July 2004, one metastatic node in the right calf had regressed and was no longer detectable by radiological imaging and positron-emission tomography. The patient was thus in complete remission and remained so during the study, until 18 mo later (September 2005) when several new metastases developed in the right lower limb. All studies have been reviewed and approved by an appropriate institutional review committee.

A2/peptide multimers and flow cytometry immunofluorescence analysis

PBMCs were obtained by density centrifugation using Ficoll-Hypaque (Pharmacia Biotech) and cryopreserved in RPMI 1640 supplemented with 40% FCS and 10% DMSO (1×10^7 – 4×10^7 cells per vial). Synthesis of PE- and allophycocyanin-labeled HLA-A*0201/peptide multimers were prepared as described previously (2, 3) with NY-ESO-1 analog peptide SLLMWITQA. Five color stains were done with PE- or allophycocyanin-HLA-A2/peptide multimers, FITC-conjugated anti-CD28, -CD27, -CD57, and -programmed death (PD)-1 (BD Biosciences), PE-conjugated anti-TCR BV8 and BV13 (Beckman Coulter) and anti-CD127 (BD Biosciences), PE-Texas Red-conjugated anti-CD45RA (Beckman Coulter), allophycocyanin/Cy7-conjugated anti-CD8 (BD Biosciences) reagents, and anti-CCR7 mAb (BD Biosciences) followed by allophycocyanin-conjugated goat anti-rat IgG Ab (Caltag Laboratories). In brief, CD8⁺ T lymphocytes were positively enriched from PBMCs using anti-CD8-coated magnetic microbeads (Miltenyi Biotec), resulting in >90% CD3⁺CD8⁺ lymphocytes. Cells were first stained with PE- or allophycocyanin-labeled multimers for 30 min at 4°C in PBS, 0.2% BSA, 50 μ M EDTA, and then with appropriate Abs (30 min, 4°C). Intracellular content of granzyme B, perforin, and Ki-67 was measured in CD8⁺ T lymphocytes without previous stimulation. After staining with appropriate mAbs, cells were fixed for 20 min at room temperature in PBS containing 1% formaldehyde, 2% glucose, and 5 mM sodium azide. Fixation was followed by permeabilization with PBS/0.1% saponin (Fluka)/0.2% BSA/50 μ M EDTA and staining with granzyme B-FITC (Hözel Diagnostika), perforin-FITC mAbs (Alexis) or Ki-67-FITC (BD Biosciences), both for 20 min at room temperature. Cells were immediately analyzed on a BD Vantage or a LSRII flow cytometer using CellQuest software (BD Biosciences). KLRG1 expression was determined by Alexa 488-conjugated anti-KLRG1 mAb 13F12F2 (22).

cDNA amplification, TCR spectratyping, sequencing, and clonotyping

Five-cell aliquots were sorted with a FACSVantage SE machine directly into wells of 96 V-bottom plates. cDNA preparation, cDNA amplification, and PCR were performed as described (23). CDR3 size of TCR transcripts and the sequences of oligonucleotides corresponding to the 22 variable segments of the TCR β -chain (based on the nomenclature proposed by Arden et al. (24)) were analyzed as follows: in brief, 8 μ l taken from 10 individually sorted and amplified 5-cell cDNA samples were pooled together to obtain total cDNA material equivalent to *ex vivo* sorted 50 cells. cDNA pools generated from circulating EM28⁺ and EM28[–] NY-ESO-1-specific T cells at different time points before and after vaccination as well as cDNA pools from NY-ESO-1-specific T cells sorted from single-cell suspension of a metastatic lymph node tissue (TILN)⁴ were subjected to individual PCR using a set of validated 5' sense fluorescent-labeled primers specific for the 22 BV subfamilies and one 3' antisense primer specific for the corresponding C gene segment (25). PCR products were then run on an automated sequencer in the presence of fluorescent size markers and data analysis was performed with the Genescan analysis software (Applied Biosystems). TCR BV-BC PCR products were directly purified and sequenced (Fasteris) when single dominant PCR peaks were identified. Two distinct sets of primers (Metabion) specific for the CDR3 region of each identified BV1, BV8, and BV13 T cell clonotype were validated and used for clonotyping PCR as recently described (13); 1) CDR3 clonotype forward and C β reverse, and 2) BV-subfamilies (BV1, BV8, or BV13) and CDR3 clonotype reverse. Forward and reverse clonotype primers are depicted as following; *BV1 clonotype 1*: 5'-AGCGTAACAGGGACAGGG G-3'; rev-5'-GCCCCCTGTCCTGTACG-3', *BV1 clonotype 2*: 5'-GTA GATGGAAGCAATCAGCC-3'; rev-5'-AAAATGCTGGGGCTGATTG C-3', *BV8 clonotype 1*: 5'-ACTTCTGTGCCAGCAACAG-3'; rev-5'-A AAGCTTCAGTACCCCTG-3', *BV8 clonotype 2*: 5'-ACTTCTGTGC CAGCAGTCTC-3'; rev-5'-AAGCTTCAGTCCCCCGAGA-3', *BV8 clonotype 3*: 5'-GTTTGGGGGCAATGAGCAG-3'; rev-5'-GAACTGC TCATTGCCCCCA-3', *BV13 clonotype 1*: 5'-GAACAGGGTTGGACG GCTAC-3'; rev-5'-GTAGCCGTCACCCCTGTT-3', *BV13 clonotype 2*: 5'-AGTTACGTAGGGGGGAAGG-3'; rev-5'-AGCTTCCCCCTAC GTAA-3', and *BV13 clonotype 3*: 5'-GACACTATAATTCACCCCTCC-3'; rev-5'-GGAGGGGTGAATTATAGTGTC-3'.

Gene expression analysis

The procedures for cDNA preparation, cDNA amplification as well as the RT-PCR were recently described in detail (23). Primers to detect CD3, CCR7, IFN- γ , granzyme B, perforin, CD94, and TNF- α mRNA transcripts were previously reported (26). Additional primers were used in the present study: *CD127/IL-7R α* : 5'-ATCTTGGCCTGTGTATGG-3'; rev-5'-AT TCTTCTAGTTGCTGAGGAAACG-3', *KLRG1*: 5'-CTTGAGCCAGG AGTTTGA-3'; rev-5'-TGGTCTCTTCATCACTGTACC-3'.

T cell cloning and culture

Multimer⁺ CD8⁺ T cell subsets (EM28⁺ and EM28[–]) were sorted by flow cytometry, cloned by limiting dilution, and expanded in RPMI 1640 medium supplemented with 8% human serum, 150 U/ml recombinant human IL-2 (rhIL-2; a gift from GlaxoSmithKline), 1 μ g/ml PHA (Sodiag) and 1×10^6 /ml irradiated allogeneic PBMC (3000 rad) as feeder cells.

Telomere fluorescence in situ hybridization and flow cytometry (flow FISH)

The average length of telomere repeats at chromosome ends in individual cells, was measured by fluorescence in situ hybridization (FISH) and flow cytometry (flow FISH) as previously reported (27, 28). Telomere length measurements were performed on 45 *in vitro* derived T cell clones sorted from EM28[–] NY-ESO-1-specific T subpopulations at various time points before and following immunotherapy, allowing the recovery of sufficient numbers of cells for flow FISH analysis. All T cell clones were expanded in identical *in vitro* culture conditions, and after a single round of stimulation, 2×10^5 cells were further processed by flow FISH. Because the average telomere fluorescence from all these clones was evaluated in the same experimental design, this allowed direct telomere comparison between each tested clone. We estimated that all clones had, on average, shortened their telomere lengths by ~1.5 kb through their *in vitro* expansion round (29). Telomere fluorescence was calculated by subtracting the mean fluorescence of the background control (no probe) from the mean

⁴ Abbreviations used in this paper: TILN, tumor-infiltrated lymph node cells; PD, programmed death; int, intermediate; EM, effector-memory; CM, central-memory.

fluorescence obtained from cells hybridized with the telomere probe after calibration with FITC-labeled fluorescent beads (Quantum TM-24 Premixed; Bangs Laboratories) and conversion into molecules of equivalent soluble fluorochrome (MESF) units. The following equation was used to estimate the telomere length in base pair: $bp = \text{MESF} \times 0.495$ (27).

LiveCount assay

Ex vivo lytic activity and Ag recognition was assessed as recently described (30) with some modifications. In brief, peptide-pulsed T2 cells (HLA-A2⁺/TAP^{-/-}) were labeled with 0.1 μM CFSE (NY-ESO-1 peptide; T2-CFSE^{low}) or with 2 μM CFSE (irrelevant peptide; T2-CFSE^{high}). A 1/1 mixture of T2-CFSE^{low} and T2-CFSE^{high} was prepared. BV8⁺ and BV13⁺ NY-ESO-1-specific CD8⁺ T lymphocytes were sorted as described above, and increasing numbers of sorted cells (63, 125, 250, 500, 1000, and 2000) were dispensed into a plate containing the peptide-pulsed T2 cells (125 cells per peptide). The percentage of specific lysis was then calculated as described by Devedre et al. (30).

IFN- γ Cytospot assay

Measurement of intracellular IFN- γ production was combined to multimer, CD28 and CD45RA labeling. 1×10^6 CD8⁺ enriched T cells (Miltenyi Biotec) were incubated for 5 h with 1×10^6 T2 cells pulsed with 10 $\mu\text{g}/\text{ml}$ irrelevant HIV-1 Pol_{476–484} (ILKEPVHGV) peptide, 10 $\mu\text{g}/\text{ml}$ cognate peptide, or 1 $\mu\text{g}/\text{ml}$ PMA/0.25 $\mu\text{g}/\text{ml}$ ionomycin, respectively. After 1 h, 10 $\mu\text{g}/\text{ml}$ brefeldin A (Sigma-Aldrich) was added. After 4 additional hours, cells were stained with multimers and Abs, fixed, permeabilized, and incubated with anti-IFN- γ -FITC in PBS/0.1% saponin for 30 min at 4°C. Cells were analyzed on a LSRII flow cytometer using CellQuest software (BD Biosciences).

CFSE proliferation assay

We incubated 2×10^6 CFSE-labeled PBMCs per ml in the presence of 10 $\mu\text{g}/\text{ml}$ cognate peptide in RPMI 1640 containing 10% human serum and 150 U/ml IL-2 for 5 days. After day 3, 4, and 5, we collected $\sim 2 \times 10^6$ cells and stained cells with multimers and Abs as described above. Cells were analyzed on a LSRII flow cytometer using CellQuest software (BD Biosciences).

Results

Dominant NY-ESO-1-specific CD8⁺ T cell clones expand and persist at high frequency ex vivo

Patient LAU 50 with advanced melanoma remained disease free for a period of 9 years before developing two new metastases, one of which was removed by surgery. Subsequently, the patient was enrolled in a vaccination trial and received monthly vaccinations with NY-ESO-1_{157–165} C165A analog peptide emulsified in IFA during 13 mo (21). During the first 3 mo of vaccination, the remaining metastasis regressed and was no longer detectable by radiological imaging and positron-emission tomography (see patient's clinical history in *Materials and Methods*). Using fluorescent HLA-A2/peptide multimers incorporating peptide NY-ESO-1_{157–165} (thereafter NY-ESO-1 multimers), we identified a high frequency (>3%) of NY-ESO-1 multimer⁺ T cells that were already detectable in the circulating CD8⁺ compartment 8 mo before the relapse of disease (Fig. 1A). This population expanded up to 10% of CD8⁺ T cells during vaccination. Of note, the high frequency values of NY-ESO-1-specific T cells observed in this particular patient represent a rare exception, because in most HLA-A2⁺ individuals cancer testis Ag-specific T cells are not detectable ex vivo (31). Multicolor flow cytometry analysis revealed that NY-ESO-1-specific T lymphocytes predominantly bore a differentiated effector-memory phenotype (EM28⁻; CD45RA⁻CCR7⁻CD28⁻), which persisted for at least 18 mo following immunotherapy (Fig. 1B; data not shown). The majority of these cells expressed intracellular granzyme B and had down-regulated CD27. In contrast, a small but yet detectable proportion ($\approx 7\%$) of the effector memory compartment contained CD28⁺ cells (designed as EM28⁺).

In several viral systems, responses to a given T cell-defined Ag often showed strong TCR selection resulting in highly restricted

TCR usage (7–12, 32). Our finding that the robust NY-ESO-1-specific T cell response is characterized by increased frequencies and differentiation into EM28⁻ cells expressing multiple effector mediators suggests a similar occurrence of oligoclonal expansions of tumor-reactive T lymphocytes. To address this point, the clonal composition of NY-ESO-1 multimer⁺ EM28⁺ and EM28⁻ ex vivo sorted fractions was analyzed by spectratyping (Fig. 1C), which measures both TCR- β -chain variable segment usage (BV) and CDR3 length heterogeneity as described recently (13). Primed EM28⁺ cells displayed large polyclonal TCR repertoires with a diverse usage of the 22 different BV families as well as high variability within CDR3 size products. In sharp contrast, EM28⁻ T cells exhibited a restricted TCR repertoire diversity with the majority of cells using BV1, BV8, or BV13 gene segments of defined CDR3 lengths. These dominant TCRs were conserved over the period during which the patient received immunotherapy (0–18 mo). TCR sequencing revealed the presence of nine distinct clonotypes; three for each of the identified TCR-BV (Table I).

Evolution of the T cell clonotypic composition during disease progression and recall responses to vaccination

To gain insight into the kinetics of each distinct BV1, BV8, and BV13 T cell clonotype over time, we first examined the proportion of the different clonotypes among ex vivo purified EM28⁺ and EM28⁻ NY-ESO-1-specific T cell subsets. To directly assess the presence or absence of particular clonotypes, we used a modified RT-PCR protocol that detects specific cDNAs after global amplification of expressed mRNAs from as few as five cells (23) and combined it with designed clonotypic primers (13). Transcript analysis revealed the presence of TCR-BV8 and -BV13 clonotypes 1 and 2 in the majority of the EM28⁺ and EM28⁻ characterized 5-cell aliquots, and these represented the most abundant clonotypes (Fig. 1, D and E; data not shown). BV8-clono1 and BV8-clono2 were dominant within blood recovered 11 mo before vaccination. The ratio BV8:BV13 was reversed 18 mo after immunotherapy, with an increase in the proportion of 5-cell samples positive for BV13 TCR clonotypes. Most strikingly, we observed the complete disappearance of BV8-clono2 TCR at the latest time point.

Increased proportions of BV13 T cell clonotypes after vaccination

Our strategy combining ex vivo cell sorting with molecular analysis of 5-cell T lymphocytes provides the identification of specific T cell clonotypes as well as insight in TCR repertoire evolution over time. However, the 5-cell approach does not allow a precise estimate of T cell frequencies. Therefore, we generated 480 T cell clones derived by in vitro limiting dilution from circulating tumor-specific EM28⁺ and EM28⁻ T cell subsets isolated at various time points. The TCR of each T cell clone was analyzed by sequencing and/or specific clonotypic PCR analysis. In agreement with the ex vivo 5-cell data, we found that over 50% of the EM28⁻ NY-ESO-1-specific T cell clones were composed of TCR BV8 clonotypes before the start of immunotherapy, whereas BV13 and BV1 clonotypes, represented 28.6 and 7.6% of the repertoire, respectively (-11 mo; Fig. 2A). Following vaccination, the proportion of cells bearing the TCR BV13 clonotypes gradually increased to 42.5% before reaching up to $\approx 60\%$ at 13 and 18 mo. In sharp contrast, the fraction of BV8-clonotypic T cell clones declined by 13 mo after treatment (23%), and we could no longer detect the BV8-clono2 at this time point (Table II). Similar shifts in the proportion of BV8 and BV13 clonotypes were found in the EM28⁺ subset (Fig. 2A; Table II). Moreover, the proportion of other and infrequent TCRs was greater within the latter subset (43–58%) than among the

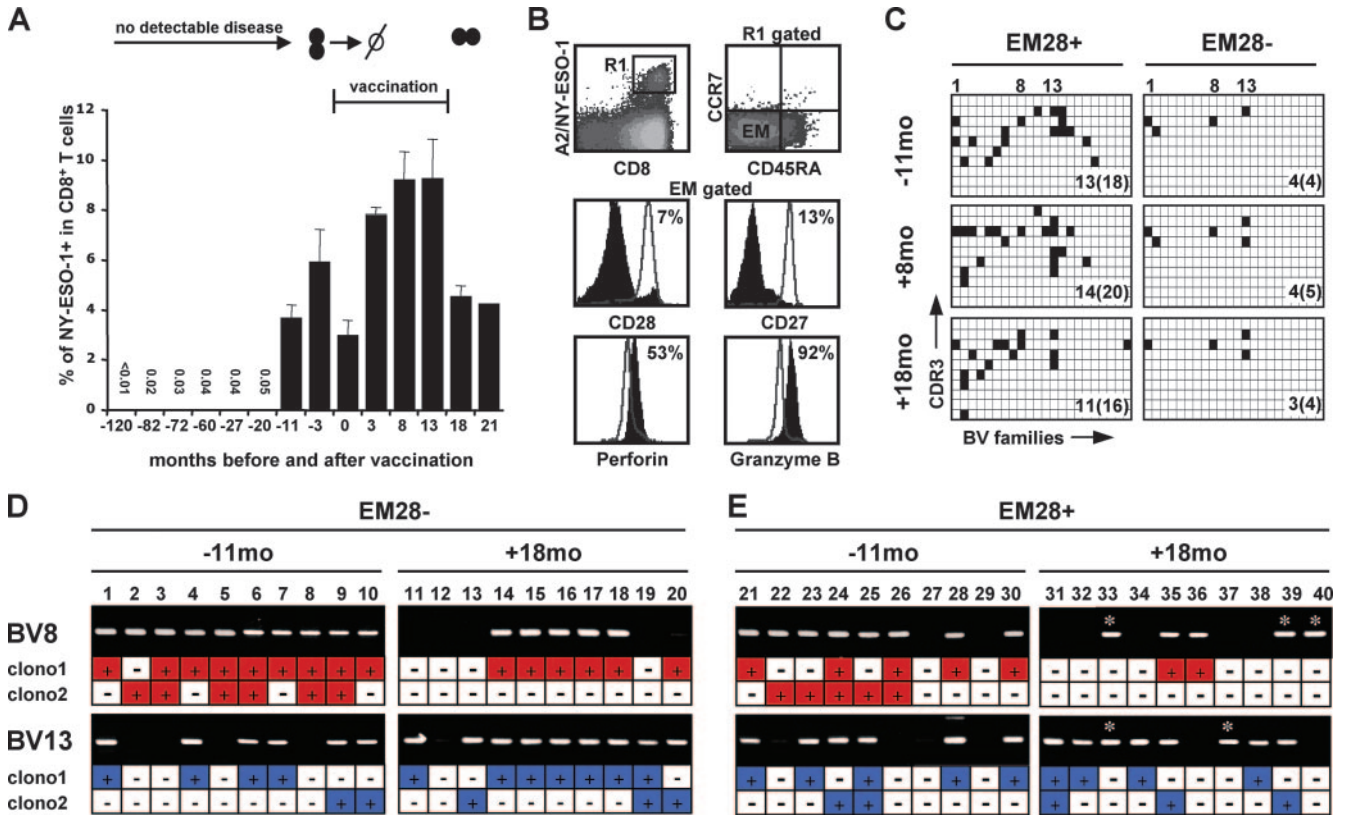


FIGURE 1. Ex vivo analysis of T cell frequency, phenotype, TCR-BV chain repertoire and TCR-BV clonotypes of circulating NY-ESO-1-specific T subsets. *A*, Percentage of multimer⁺ cells of circulating CD8⁺ T cells over time. Occurrence of two metastases (−3 mo) and regression of one remaining after surgery (+3 mo) are indicated by filled circles and an opened circle, respectively. The time period of 12 monthly vaccinations is indicated. *B*, For characterization of T cell differentiation, CD8⁺NY-ESO-1⁺ T cells (R1 gated) were analyzed ex vivo by flow cytometry for their cell surface expression of the tyrosine phosphatase CD45RA and the homing chemokine receptor CCR7. The proportion of CD28[−], CD27[−], perforin[−], and granzyme B⁺ cells among multimer⁺CD45RA[−]CCR7[−] (EM gated) specific T cells was determined by immunofluorescence (−11 mo; black histograms). The reference for CD28 and CD27 negativity, and granzyme B and perforin positivity is based on the signal obtained after gating on bulk CD8⁺CD45RA⁺CCR7⁺ naive T cells known to be CD28⁺CD27⁺perforin[−]granzyme B[−] cells (open histogram). *C*, cDNA pools (50 cells) generated from EM28⁺ and EM28[−] NY-ESO-1-specific T cells sorted from circulating CD8⁺ T cells at different time points were amplified by PCR using 22 BV-specific primers and subjected to electrophoresis on an automated sequencer. Each BV subfamily (*x*-axis) was analyzed for the presence of amplified BV-CDR3-BC products of defined CDR3 size (*y*-axis), and displayed by black squares on a grid. The columns corresponding to the BV1, BV8, and BV13 subfamilies are labeled. The figures inserted in each grid indicate the total number of BV subfamily gene segment usage vs the total number of all amplified BV-CDR3-BC products within each positive BV subfamily. *D* and *E*, Unique primers corresponding to the CDR3 gene segment of each identified TCR clonotype were designed and validated (see *Materials and Methods*). Clonotypic PCR was performed on cDNA obtained from individually sorted 5-cell samples of NY-ESO-1-specific EM28[−] (*D*; #1–20) and EM28⁺ (*E*; #21–40) CD8⁺ T cells isolated before (−11 mo) and after (+18 mo) vaccination (*n* = 10). Samples yielding detectable clonotypic-specific signals are depicted in color ⁺. Gene expression patterns of global TCRs BV8 and BV13 are also shown. BV8-clono1, BV8 clonotype 1; BV8-clono2, BV8 clonotype 2; BV13-clono1, BV13 clonotype 1; BV13-clono2, BV13 clonotype 2. The asterisk (*) corresponds to samples expressing nonclonotypic BV8 or BV13-TCR gene segments. As this was mostly observed in EM28⁺ cells, these data confirm increased TCR repertoire heterogeneity in EM28⁺ cells compared with the EM28[−] compartment.

Table I. TCR-BV usage of A2/NY-ESO-1_{157–165} specific T cell clonotypes from patient LAU 50

Clonotype	BV ^a	CDR3β	BJ	CDR3 Size
Clono1 ^b	BV1S1	CAS SVTGTGGG	FFG (BJ2.1)	8 aa
Clono2	BV1S1	CAS SVDGSNQQQ	HFG (BJ1.5)	9 aa
Clono3	BV1S1	CAS SVTGTEEA	FFG (BJ1.1)	8 aa
Clono1 ^b	BV8S2	CAS QQGGTEA	FFG (BJ1.1)	7 aa
Clono2	BV8S2	CAS SLGGTEA	FFG (BJ1.1)	7 aa
Clono3	BV8S2	CAS SLGGNEQ	FFG (BJ2.1)	7 aa
Clono1 ^b	BV13S1	CAS RTGLDGY	TFG (BJ1.2)	7 aa
Clono2	BV13S1	CAS SYVGGKAEA	FFG (BJ1.1)	9 aa
Clono3	BV13S6	CAS SLTGHYNSPL	HFG (BJ1.6)	10 aa

^a The TCR-BV nomenclature used was according to Arden and colleagues (24).
^b Clonotypes recently identified by Le Gal et al. (38).

EM28[−] cells (5–10%). The proportions of NY-ESO-1-specific BV8 and BV13 T cell clonotypes 1 and 2 were calculated as percentages of circulating CD8⁺ T lymphocytes (Fig. 2*B*). A drastic increase in frequencies of both BV13-clono1 and BV13-clono2 T cells was observed during immunization, reaching up to 3.1 and 2.2%, respectively. In contrast, the proportion of BV8-clono1 and BV8-clono2 T cells diminished over time, which became particularly evident at 18 mo. Similar kinetics were observed when the proportion of individual BV8 and BV13 clonotypes was adjusted to the total counts of leukocytes (data not shown).

Finally, we also used mAbs directed against the variable region of TCR BV8 and BV13 to sort 5-cell aliquots from BV8^{high} and BV8[−], as well as BV13^{high}, BV13^{int}, and BV13[−] NY-ESO-1-specific EM28[−] T cells ex vivo (Fig. 2*C*). A convenient feature of the anti-BV13 mAb reactivity allowed us to clearly discriminate between bright cells that exclusively

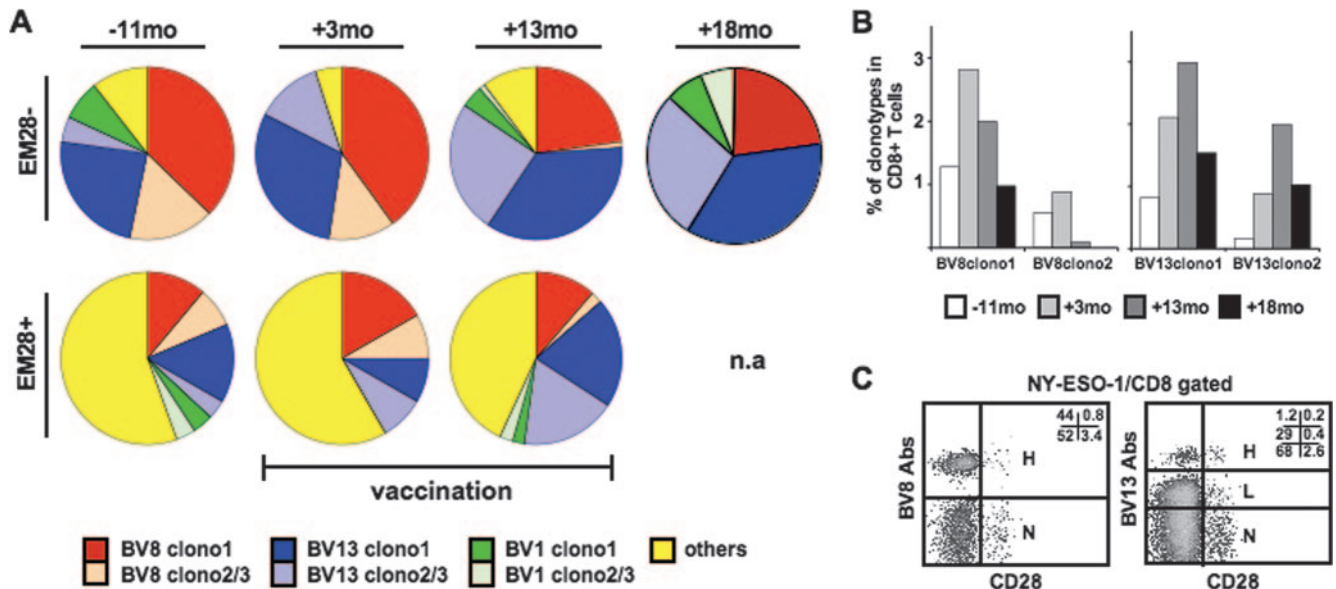


FIGURE 2. Quantification of distinct TCR-BV1, -BV8, and -BV13 NY-ESO-1-specific T cell clones using clonotypic primers. **A**, Clonotypic PCR was performed on T cell clones in vitro generated from circulating tumor-specific EM28⁺ ($n = 122$) and EM28⁻ ($n = 324$) T cell subsets at various time points (-11 mo to $+18$ mo). The same set of clonotypic primers as described in *Materials and Methods* was used. Results are presented as percentage of BV8 (red), BV13 (blue), and BV1 (green) T cell clonotypes, and of nonclonotypic (yellow) T cells in EM28⁻ and EM28⁺ tumor-specific T cells, respectively (see Table II). **B**, Percentage of total BV8-clono1, BV8-clono2, BV13-clono1, and BV13-clono2 NY-ESO-1-specific T cells among the circulating CD8⁺ compartment over time. **C**, The proportion of BV8⁺ and BV13⁺ cells within EM28⁺ and EM28⁻ multimer⁺CD45RA⁻CD8⁺ T cells was determined by immunofluorescence (at time point 11 mo before the start of immunotherapy). Of note, EM28⁺ and EM28⁻ T cells comprising low and high staining intensities were observed when using the anti-BV13 mAb.

comprised the BV13-clonotype 2 and dim cells selectively containing the BV13-clonotype 1 (Table III). Moreover, all BV8-clono1 and BV8-clono2 were comprised within the BV8⁺ cells whereas none were detectable in the BV8⁻ fraction of the cells. The proportion of BV8-clono1/clono2, BV13-clono1 and BV13-clono2 T cells represented 44, 29, and 1.2%, respectively, of total NY-ESO-1-specific EM28⁻ T cells (Fig. 2C). These results are in excellent agreement with the data from the T cell clones (Fig. 2A; Table II), indicating that our in vitro T cell cloning approach did not introduce major biases and can thus be efficiently used to assess clonotype frequencies among Ag-specific CD8⁺ T cells.

Predominance of BV13 T cell clonotypes in a metastatic lymph node

We next evaluated the TCR usage of NY-ESO-1-specific T cell subsets within a metastatic lymph node, resected 3 mo before the start of peptide vaccination (-3 mo). Most tumor-specific T cells exhibited the effector-memory CD45RA⁻CCR7⁻ phenotype, with a dominant fraction of these cells that had down-regulated CD28 and CD27, and up-regulated granzyme B and perforin (Fig. 3A). As their counterparts in peripheral blood samples, TCR-BV diversity in the multimer-specific EM28⁻ T cell subpopulation

Table II. *Estimated proportions of TCR-BV1, -BV8 and -BV13 clonotypes among NY-ESO-1-specific T cell subsets over time and in a metastatic lymph node*

Sample	No. of Clones	BV1 Clonotyping			BV8 Clonotyping			BV13 Clonotyping			Others
		Clono1	Clono2	Clono3	Clono1	Clono2	Clono3	Clono1	Clono2	Clono3	
EM28 ⁺											
-11 mo	54 ^a	3.7 ^b	0.0 ^b	3.7 ^b	11.1 ^b	0.0 ^b	7.4 ^b	14.8 ^b	1.9 ^b	1.9 ^b	55.6 ^b
+3 mo	24	0.0	0.0	0.0	16.7	8.3	0.0	8.3	8.3	0.0	58.3
+13 mo	44	2.3	2.3	0.0	11.4	2.3	0.0	20.5	18.2	0.0	43.2
+18 mo	na	na	na	na	na	na	na	na	na	na	na
EM28 ⁻											
-11 mo	105	7.6	0.0	0.0	37.1	16.2	0.0	23.8	4.8	0.0	10.5
+3 mo	40	0.0	0.0	0.0	40.0	12.5	0.0	30.0	12.5	0.0	5.0
+13 mo	96	4.2	1.0	0.0	22.9	1.0	0.0	35.4	25.0	0.0	10.4
+18 mo	83	7.2	6.0	0.0	22.9	0.0	0.0	36.1	24.1	3.6	0.0
TILN											
EM28 ^{low}	53	11.3	1.9	0.0	1.9	1.9	9.4	15.1	20.8	3.8	34.0
EM28 ⁻	17	17.6	0.0	0.0	17.6	11.8	0.0	41.2	5.9	0.0	0.0

^a Total number of in vitro generated T cell clones analyzed for their TCRs by sequencing and/or clonotyping.

^b Proportion of each distinct BV1, BV8, and BV13 clonotype in percentage. na, not applicable. TILN (-3 mo). -11 mo to $+18$ mo represents blood samples retrieved at various time points before and after vaccination.

Table III. *Ex vivo estimated proportions of TCR-BV8 and -BV13 clonotypes among BV8- and BV13-positive NY-ESO-1-specific EM28⁻ sorted 5-cell samples^a*

Sorted Sample	BV1 Expression		BV8 Expression		BV13 Expression		
	BV1 ^b	BV8 ^b	Clono1 ^c	Clono2 ^c	BV13 ^b	Clono1 ^c	Clono2 ^c
BV8 ^{high}	2/15	15/15	14/15	14/15	0/15	nd	nd
BV8 ⁻	10/20	0/20	nd	nd	19/20	nd	nd
BV13 ^{high}	0/13	0/13	nd	nd	13/13	0/13	13/13
BV13 ^{low}	0/14	1/14	nd	nd	14/14	14/14	0/14
BV13 ⁻	14/20	20/20	nd	nd	5/20	5/20	0/20

^a All shown data are from PBMC collected from a lymphocytopheresis withdrawn 11 mo before vaccination. nd, not determined. Of note, most TCR-BV1 expressing T cells were detected in the sorted BV8- and BV13-negative fraction of the 5-cell samples.

^b Proportion of positive TCR-BV1, -BV8, or -BV13 subfamilies per 5-cell aliquots.

^c Proportion of positive clonotypes per 5-cell aliquots.

was limited with preferential presence of BV1-, BV8-, and BV13-expressing cells (Fig. 3B). Again, the TCR repertoire in the EM28^{low/+} fraction was more diverse than in the EM28⁻ subset. We further investigated the proportion of each T cell clonotype by *ex vivo* sorting of 5-cell samples (Fig. 3C) and analysis of *in vitro* generated T cell clones (*n* = 70; Fig. 3D). All of the clonotypes identified within the circulating NY-ESO-1-specific CD8⁺ T cells were also found in the metastatic tissue. In contrast to the data obtained from peripheral blood (-11 mo; Fig. 2A), the BV13 clones were predominant in both EM28⁺ and EM28⁻ T cell subpopulations, whereas BV8 T cell clonotypes were represented at reduced frequencies (Table II). This dominance was particularly marked within the EM28⁺ compartment. Altogether, these results provide molecular evidence that the prevalence for BV13 clonotypes observed within multimer-specific CD8⁺ T lymphocytes of a metastatic lymph

node resected 3 mo before the start of vaccination (-3 mo) precedes the BV13>>BV8 ratio attained about 2 years later in the peripheral blood (+18 mo; Fig. 2A).

Rapid telomere shortening within BV13 T cell clonotypes contrasts with stabilized telomeres in BV8 clonotypes over time

We next measured the turnover of distinct NY-ESO-1-specific T cell clonotypes before and after immunotherapy (Fig. 4A). Because telomeres progressively shorten as a function of cell division, telomere length is a powerful indicator of the *in vivo* replicative history of lymphocytes (27). We observed a drastic reduction in the mean telomere fluorescence of BV13 T cell clonotypes over time, that corresponded to a loss of ~2.4 kb, indicating extensive *in vivo* proliferation. Telomere shortening seemed coincident with immunotherapy, because BV13 clonotypes from the metastatic lymph

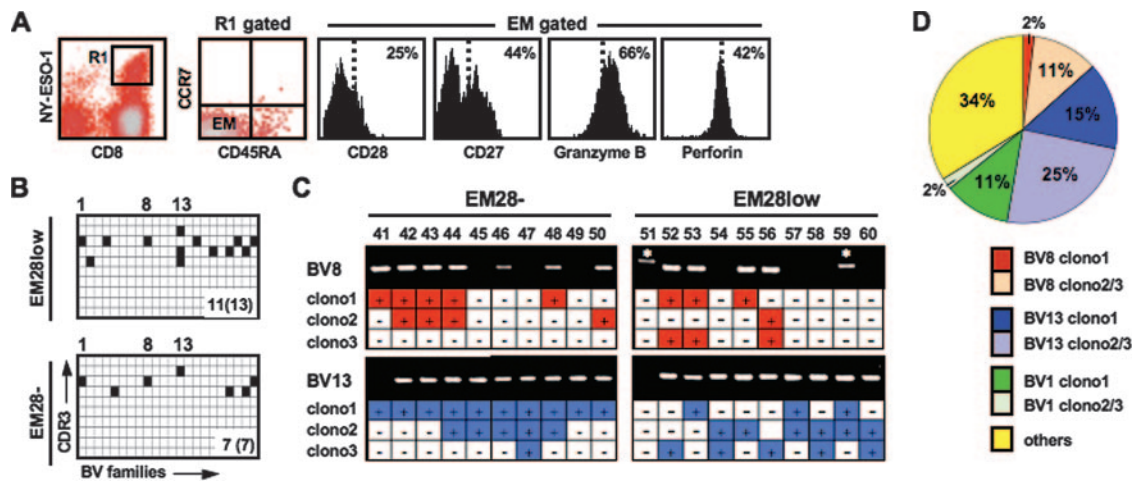


FIGURE 3. *Ex vivo* analysis of T cell frequency, phenotype, TCR-BV chain repertoire, and TCR-BV clonotypes of NY-ESO-1-specific T cell subsets from metastatic tissue. **A**, An inguinal metastatic lymph node (TILN) was surgically removed 3 mo before immunotherapy, and CD8⁺NY-ESO-1⁺-specific T cells (R1 gated) were characterized *ex vivo* by flow cytometry for their cell surface expression of CD45RA and CCR7. The proportion of CD28-, CD27-, granzyme B-, and perforin-positive cells among multimer⁺CD45RA⁺CCR7⁻ (EM gated)-specific T cells was determined by immunofluorescence. The reference for CD28 and CD27 negativity, and granzyme B and perforin positivity is based on the signal obtained after gating on bulk CD8⁺CD45RA⁺CCR7⁺ naive T cells (dotted line). **B**, cDNA pools (50 cells) generated from EM28^{low} and EM28⁻ NY-ESO-1-specific T cells sorted from freshly prepared single-cell suspensions of the metastatic TILN were amplified by PCR using 22 BV-specific primers and subjected to electrophoresis on an automated sequencer. The columns corresponding to the BV1, BV8, and BV13 subfamilies are labeled. Total numbers of TCR-BV usage (x-axis) comprising all amplified BV-CDR3-BC size product (y-axis) are indicated in each grid. **C**, Clonotypic PCR was performed on cDNA obtained from individually sorted 5-cell samples of NY-ESO-1-specific EM28⁻ (#41–50) and EM28^{low} (#51–60) CD8⁺ T cells isolated from the metastatic TILN (*n* = 10). Samples yielding detectable clonotypic specific signals are depicted in color (+). Gene expression patterns of global TCRs BV8 and BV13 are also shown. The asterisk (*) corresponds to samples expressing nonclonotypic BV8 or BV13-TCR gene segments. **D**, Clonotypic PCR was performed on *in vitro* generated T cell clones from EM28^{low} tumor-specific T cells isolated from TILN (*n* = 53). Results are presented as percentage of BV8 (red), BV13 (blue), and BV1 (green) T cell clonotypes, and of nonclonotypic (yellow) T cells. The same set of clonotypic primers as described in *Materials and Methods* was used.

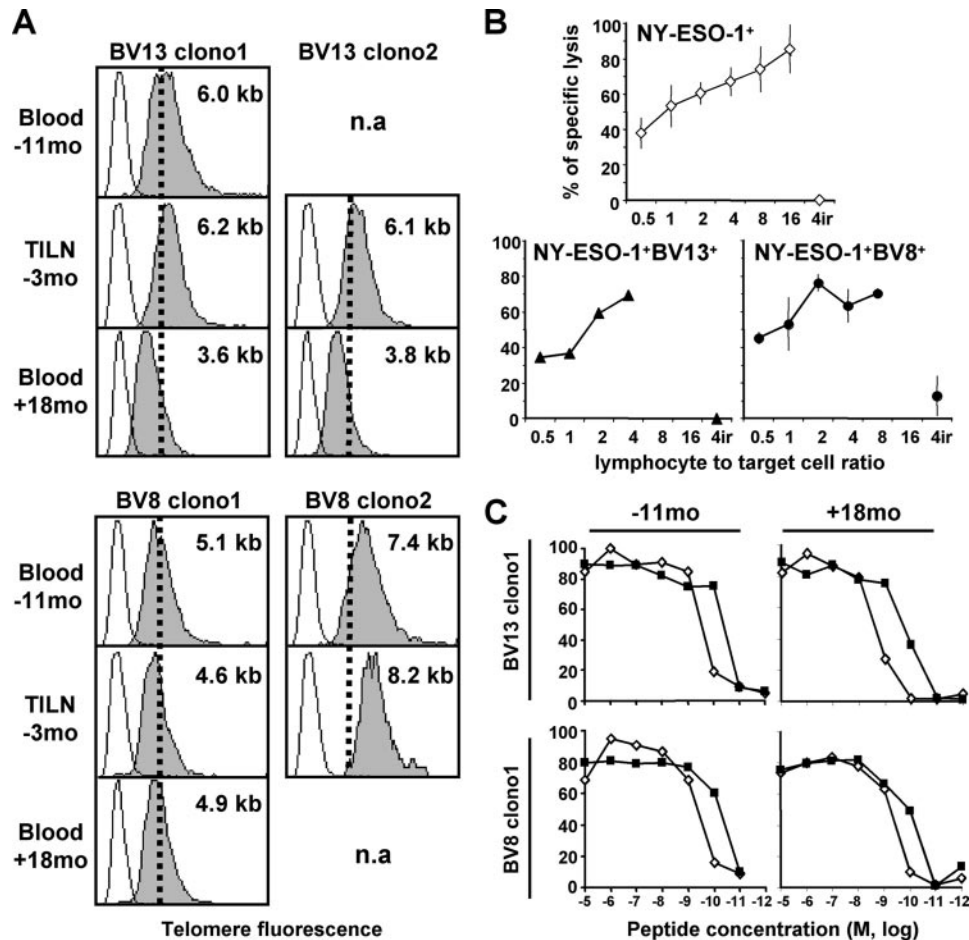


FIGURE 4. Analysis of replicative history and ex vivo cytotoxicity. *A*, Analysis of telomere fluorescence was performed by flow FISH on 45 T cell clones derived from circulating EM28⁻ NY-ESO-1-specific T cells isolated at different time points and from TILN. Each T cell clone was assessed for its TCR clonotype by clonotypic PCR. As several clones were tested per time point, tissue (PBMC and TILN), and clonotype, a representative example of each was chosen (total of 41 tested clones). The dotted line was arbitrarily set at the mean telomere signal obtained for BV8-clonotype 1 (-11 mo) and allows the direct comparison between samples. The mean average telomere fluorescence from several analyzed T cell clonotypes is depicted in kilobase (kb). Of note, telomere fluorescence of BV13-clono2 (-11 mo) and BV8-clono2 (+18 mo) T cell clonotypes could not be assessed, as no (BV8-clono2) or only limited numbers (BV13-clono2) of T cell clones could be obtained due to their low frequency within the EM28⁻ compartment (see Table II). One experiment of two is shown. *B*, Ex vivo assessment of cytotoxicity using the LiveCount assay (30). Increasing numbers of total, BV8⁺ or BV13⁺ NY-ESO-1-specific CD8⁺ T cells (-11 mo) were sorted and coincubated with an equal number of NY-ESO-1 peptide pulsed T2-CFSE^{low} and irrelevant (ir) peptide pulsed T2-CFSE^{high} cells at the indicating E:T cell ratios. *C*, The relative TCR avidity was compared using T2 target cells (HLA-A2⁺/TAP^{-/-}) pulsed with graded concentrations of either analog NY-ESO-1₁₅₇₋₁₆₅ peptide (SLLMWITQA; filled squares) or native NY-ESO-1₁₅₇₋₁₆₅ peptide (SLLMWITQC; unfilled diamonds). Representative examples of percentage of specific killing by BV8- and BV13-clonotype 1 T cells before (-11 mo) and after (+18 mo) peptide vaccination are depicted ($n = 103$ clones). Similar data were obtained for BV8- and BV13-clonotype 2 T cells (data not shown).

node (-3 mo) displayed similar average telomere lengths compared with the clones isolated from the earliest blood sample before vaccination (-11 mo). Despite its subsequent disappearance, the BV8-clono2 displayed the brightest telomere signal, and no telomere loss was observed within the BV8-clonotype 1 subpopulation over time. Altogether, our data indicate that several tumor-specific T cell clones may persist over extended periods of time in vivo, likely reflecting the repetitive triggering by Ag derived from tumor cells or vaccination. Others eventually disappear from the blood, but this is not associated with a state of replicative senescence.

EM28⁻ T cell clonotypes mediate efficient ex vivo killing, produce IFN- γ and retain proliferative capacity upon antigenic stimulation

The finding of distinct kinetics among NY-ESO-1-specific BV subpopulations over time prompted us to assess their ex vivo cy-

tolytic activity using a novel flow cytometry-based cytotoxic assay (30). As depicted in Fig. 4*B*, BV8⁺ and BV13⁺ NY-ESO-1-specific T lymphocytes efficiently and similarly killed NY-ESO-1-peptide pulsed T2 cells. These data are in agreement with chromium release assays performed with EM28⁻ derived BV8⁺ and BV13⁺ T cell clones ($n = 103$), where we found similar efficiency by the different clonotypes to recognize NY-ESO-1 expressing autologous tumor cells and T2 cells labeled with titrated amounts of NY-ESO-1 peptides (Fig. 4*C*; data not shown). Efficiency of target cell lysis apparently remained stable over time, as we obtained similar results with clones of BV8 and BV13 T cell clonotypes 1 and 2 generated from blood samples retrieved before (-11 mo) or after (+18 mo) immunotherapy (Fig. 4*C*; data not shown).

We next investigated whether BV8 and BV13 T cell clonotypes differed in the expression of molecules involved in T cell effector, survival, or regulatory functions. A similar proportion of 5-cell samples containing ex vivo detectable IFN- γ , TNF- α , granzyme B,

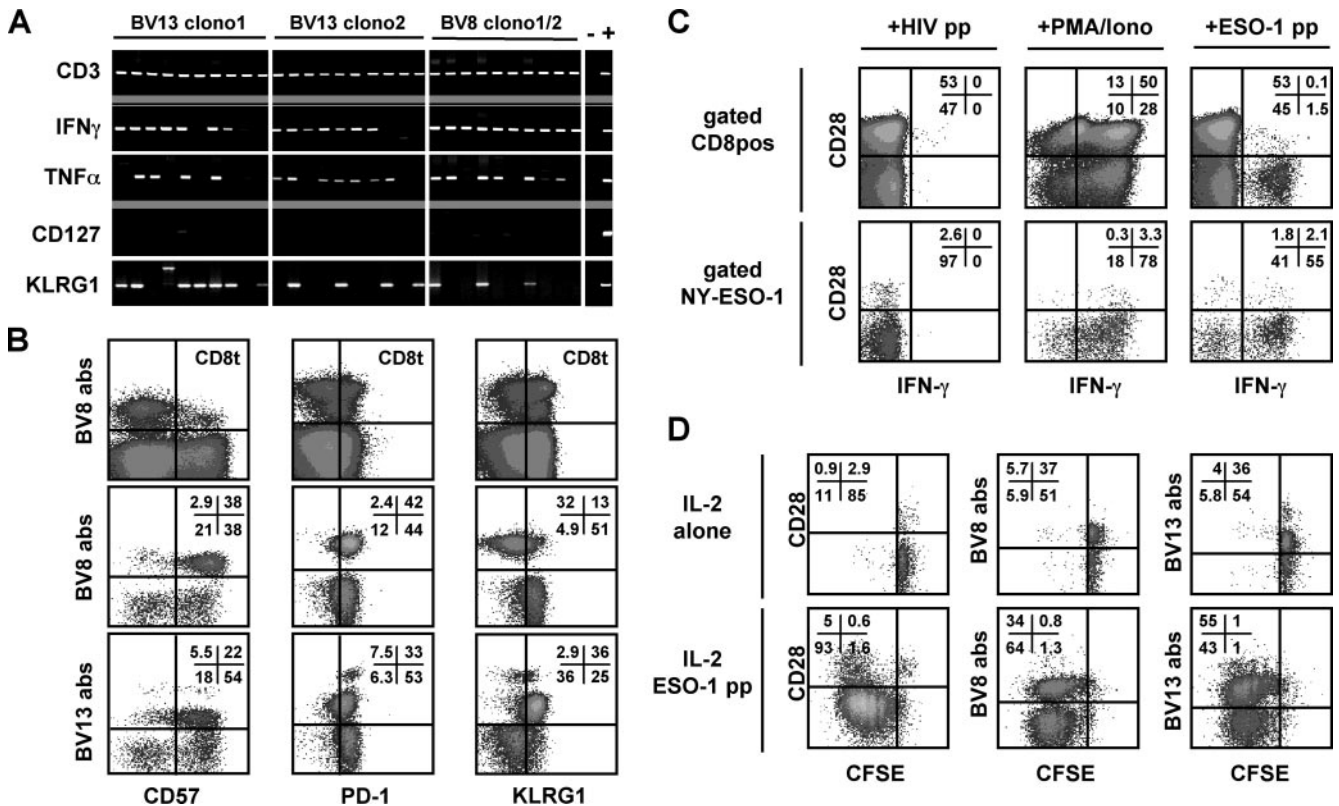


FIGURE 5. Ex vivo expression of mediators involved in T cell effector, survival and regulatory functions within clonotypes. *A*, Gene expression analysis was performed on cDNA obtained from individually sorted 5-cell samples of BV13^{high} (BV13-clono2), BV13^{low} (BV13-clono1), and BV8^{high} (mix of BV8-clono1 and BV8-clono2) EM28⁻ NY-ESO-1-specific T cells as described in Fig. 2C. All shown data are from PBMC collected from a lymphocytapheresis withdrawn 11 mo before vaccination (-11 mo). PCR products designed for CD3, IFN- γ , TNF- α , CD127, and KLRG1 mRNA transcript analyses are depicted. Data from 10 independent 5-cell aliquots are shown; negative (-) and positive (+) controls. *B*, The proportion of CD57⁻, PD-1⁻, and KLRG1⁻ cells within BV8⁺ and BV13⁺ (multimer⁺CD8⁺CD45RA⁻) T cells was determined by multiparameter flow cytometry. Quadrants are set according to the internal control staining obtained from bulk multimer⁻CD8⁺ T lymphocytes. Of note, we were unable to determine the proportion of CD127⁺ cells within BV8⁺ and BV13⁺ specific T cells due to the limitation of available mAb combinations. *C*, IFN- γ production by NY-ESO-1-specific CD8⁺ T cells (-11 mo). Isolated CD8⁺ T cells were stimulated with irrelevant HIV-1 peptide (*left*), PMA/ionomycin (*middle*), or cognate peptide (*right*). Quadrants are set according to the internal control staining obtained from whole CD8⁺multimer⁻ T cells (see *top panels*). *D*, Representative dot plots (multimer⁺CD8⁺CD45RA⁻ gated cells) of a 5-day stimulation assay performed on CFSE-labeled PBMCs in the presence of IL-2 alone or IL-2 plus cognate peptide. At day 5, 2×10^6 cells were labeled with NY-ESO-1-specific multimers, CD28 or TCR-BV8 or -BV13 Abs, and analyzed by flow cytometry. A representative experiment of three is shown (*C* and *D*).

perforin, and C-type killer cell lectin-like receptor CD94 transcripts, was found in both BV clonotypes (Fig. 5A; data not shown). These clones displayed a highly differentiated phenotype, because a majority of the cells expressed CD57 whereas having down-regulated CD127 (IL-7R α), CD27, and L-selectin (CD62-L) expression (Fig. 5B; data not shown). Moreover, BV8⁺ and BV13⁺ NY-ESO-1-specific T cells expressed similar levels of PD-1. Surprisingly, the number of samples positive for KLRG1 mRNA, another killer cell lectin-like receptor, was much higher in both BV13-1 and BV13-2 clonotypes than in BV8 clonotypes (Fig. 5A), correlating with the analysis of KLRG1 protein expression by FACS (Fig. 5B). Indeed, the majority of NY-ESO-1-specific BV13⁺ cells expressed KLRG1 (>80%), whereas only 15–20% of BV8 clonotypes expressed the protein. Similar profiles of PD-1 and KLRG1 protein expression were observed 8 mo after immunotherapy (data not shown).

A significant proportion of NY-ESO-1-specific T cells produced IFN- γ after short-term antigenic challenge as well as after non-specific PMA/ionomycin stimulation (Fig. 5C). As observed previously, most of the IFN- γ -secreting cells stimulated by the cognate peptide were differentiated EM28⁻ cells. Finally, we

stimulated CFSE-labeled PBMC with IL-2 alone or IL-2 plus NY-ESO-1 peptide to determine the proliferative potential of NY-ESO-1-specific CD8⁺ T cells (Fig. 5D). We found an important fraction of EM28⁺ and EM28⁻ Ag-specific T cells as well as of BV8⁺ and BV13⁺ Ag-specific T cells that divided in response to antigenic stimulation. This is in line with the small proportion of ex vivo NY-ESO-1-specific EM28⁺ and EM28⁻ T cell clonotypes that expressed low, but readily detectable levels of Ki-67, indicating that cycling cells are present in both compartments (Fig. 6A). Collectively, our data show that tumor-specific EM28⁻ BV8 and BV13 T cell clonotypes are composed of differentiated cells with strong and efficient effector properties, although retaining their proliferative potential.

Preferential expression of CD127/IL7R α but not of PD-1 by EM28⁺ T cells

We monitored CD27, granzyme B, perforin, CD127, PD-1, and KLRG1 expression in combination with CD28 (Fig. 6). An important fraction of tumor-specific EM28⁺ T cells expressed CD27 (87%) and CD127 (60–70%), whereas they expressed granzyme B (36%), perforin (27%), and PD-1 (20–30%) at much lower levels

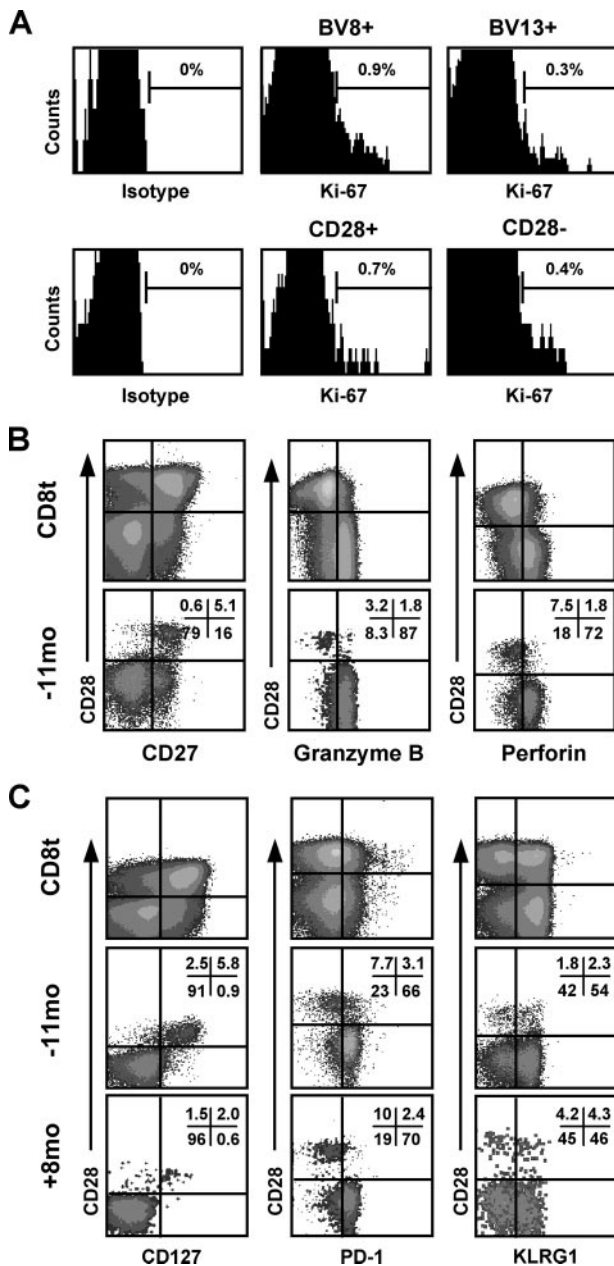


FIGURE 6. Ex vivo expression of mediators involved in T cell proliferation, survival, effector, and regulatory functions within EM28⁺ and EM28⁻ subsets. **A**, Analysis of Ki-67 expression (a marker of proliferation) within circulating BV8⁺ or BV13⁺ (*top panels*) and EM28⁺ or EM28⁻ (*bottom panels*) specific CD8⁺ T cells (-11 mo). The gating for Ki-67 positive cells is based on isotype control stainings. One representative experiment of three is shown. **B** and **C**, Analysis of CD27, CD127, PD-1, and KLRG1 cell surface expression on EM28⁺ and EM28⁻ (multimer⁺CD8⁺CD45RA⁻) T cell subsets before (-11 mo) and after (+8 mo) vaccination. The proportion of granzyme B- and perforin-positive cells in EM28⁺ and EM28⁻ multimer⁺CD8⁺CD45RA⁻ specific T cells was also determined. For comparison, stainings on whole multimer⁻CD8⁺ T lymphocytes (CD8t) are depicted.

than EM28⁻ cells (70–90%). In contrast, the same proportion of KLRG1⁺ cells was observed within EM28⁺ and EM28⁻ compartments (\approx 50%). Altogether, our data show that unlike tumor-specific EM28⁻ T cells that are closely related to effector-type cells, the EM28⁺ Ag-specific cells share functional features with memory lymphocytes. As the latter subset contains all identified tumor-specific T cell clonotypes, it may potentially serve as a pool for

clonotypic T cells that can differentiate, expand, and mediate effector functions when required. Finally, KLRG1 expression is associated with distinct tumor-specific CD8⁺ T cell clonotypes, rather than with their functional differentiation status.

Discussion

It is now well established that cancer patients often acquire Ag-specific T cell responses to various targets. In a few cases it is even possible to directly study the population of responding T cells because of the presence of a particularly strong response. Insight into the magnitude of such responses has been gradually gained mainly because of the use of MHC/peptide multimers that allow the direct identification and isolation of specific T cells. However, a truly detailed knowledge of the ex vivo dynamics of individual T cell clones is still lacking. Here, we present an extensive study on the functional and proliferative potential of a dominant CD8⁺ T cell response directed against NY-ESO-1, a well-known tumor Ag, on analyzing individual T cell clonotypes in tumor tissue and peripheral blood over a prolonged period of time.

We could identify two functionally distinct populations of multimer⁺ T cells. The major population making up to 90% of the cells displayed the hallmarks of highly differentiated and active effector T cells (Fig. 1). Indeed, beside down-regulating lymph node homing (CCR7 and CD62L) and costimulatory (CD28 and CD27) receptors, these repetitively stimulated T cells (also designated as EM28⁻) down-regulated IL-7R α (involved in pro-survival/homeostatic signals delivered by IL-7) while up-regulating NK-like receptors such as CD57 and CD94, as well as PD-1, an inhibitory receptor. This dominant subset was mostly composed of nine expanded T cell clonotypes incorporating variable TCR-BV domains from only three subfamilies (BV1, BV8 and BV13). The other relatively minor population (EM28⁺), representing between 5 and 10% of the NY-ESO-1-reactive CD8⁺ T lymphocytes, was also differentiated with features consistent with a resting memory state (CD28⁺CD27⁺CD127⁺PD-1⁻granzymeB⁻perforin⁻) (26, 33, 34). The 9:1 ratio between these two subsets prevailed over the entire observation period.

A remarkably and somewhat surprising finding was that all NY-ESO-1-specific T cell clonotypes were found to be present within the tiny memory multimer⁺ T cell population, despite their otherwise large TCR heterogeneity (Fig. 2). Thus, our results indicate that such population serves as a reservoir for clonal expansion of tumor-reactive dominant effector T cell responses with efficient effector properties. This view is supported by two recent studies reporting that murine TCR repertoires of both central-memory (CM; CD62L^{high}) and effector-memory (EM; CD62L^{low}) Ag-specific CD8⁺ T cells were largely overlapping (35, 36). Kedzierska and coworkers (36) also showed that the memory CD62L^{high} T cell repertoire was more diverse, thus preserving clonal diversity, and proposed that the “best-fit” TCRs were selected from the CM subset into the EM subset. The very limited human data published so far indicated that T cell clonotypes can indeed be shared by CM and EM cells (37), but more studies are necessary to precisely describe human T cell differentiation at the clonotypic level.

Another major finding is that at least three of the dominant BV1, BV8, and BV13 T cell clonotypes displayed long-term in vivo persistence for up to 6 years (38). This is consistent with the capacity of the NY-ESO-1-specific EM28⁺ and EM28⁻ T cells to proliferate when exposed to cognate Ag (Fig. 5). However, despite long-term persistence, we observed a progressive shift in the proportion of dominant clonotypes with an increase in BV13 T cells, whereas BV8 populations declined over time in vivo (Fig. 2). Such changes were coincident with repeated peptide vaccination and

with a 2-fold expansion of the multimer⁺ population. Fluctuations in the TCR repertoire of Ag-specific CD8⁺ T cell populations have also been reported during primary HIV infection (39), in HIV infected individuals with partial control of viremia (19), as well as in an healthy subject during the first year of EBV infection (40). Whether the decline in frequency of particular T cell clones is permanent or whether it represents a temporary or random fluctuation of the TCR repertoire remains still unclear, and deserves further in-depth analyses.

Our data revealed that the BV8-clonotype 2 cell subpopulation was undetectable at the latest time point analyzed (+18 mo), despite displaying relatively long average telomere lengths (Fig. 4). This indicates that the differential evolution observed between BV8 and BV13 T cell clonotypes cannot be attributed to replicative senescence due to the presence of critically short telomeres (27). Moreover, we found a rapid loss of telomere length within these clonotypes, corresponding to a 20-fold increased turnover rate when compared with average telomere shortening in total CD8⁺ T cells associated with aging (28). The results reported here support the view that the loss of the BV8 clonotype 2 is likely due to dilution upon clonal expansion of the BV13 clonotypes. However, one cannot formally exclude that the progressive deletion of BV8 T cell clonotypes is associated with activation-induced cell death following repetitive triggering by Ag derived from tumor cells or vaccination. Because apoptosis is rapidly induced upon TCR triggering, this question remains difficult to assess experimentally, because MHC-peptide-multimers are required to study T cells in the context of natural TCR repertoires, but multimers trigger TCRs and thus promote apoptosis. Intriguingly, the BV13:BV8 ratio attained by the end of the observation period in the circulating lymphocyte compartment (+18 mo) was already present in the NY-ESO-1-specific T cell population isolated from a tumor infiltrated lymph node resected 21 mo earlier, at a time predating the instauration of therapeutic vaccination (Fig. 3). Due to the low frequencies of circulating EM28⁺ Ag-specific T cells, we were unable to assess the telomere lengths of such cells. Future work involving the careful evaluation of their replicative history combined to their cell cycle status are needed to fully elucidate the role of EM28⁺ cells in CD8⁺ T cell differentiation, eventually leading to the generation of differentiated EM28⁻ cells.

One question raised by our data concerns the biological parameters that may trigger the preferential selection of BV13 T cell clonotypes over time. The avidity of the TCR for MHC/peptide complexes is unlikely to be involved because the different BV8 and BV13 clonotypes recognized and killed autologous NY-ESO-1 tumor cells and peptide-pulsed T2 cells with similar functional avidity (Fig. 4; data not shown). In addition, immunotherapy had no detectable impact on the functional avidity of BV8 and BV13 T cell clonotypes, because the clones shared similar killing efficacy, whether the cells were retrieved before or after the start of peptide vaccination. High levels of KLRG1 expression were seen on chronically activated EBV- and CMV-specific CD8⁺ T lymphocytes, and to a lesser extent on T cells specific for influenza, a resolved infection without a latent stage (41, 42). In line with these results, we found that a significant proportion of NY-ESO-1-specific EM28⁺ and EM28⁻ T lymphocytes expressed KLRG1 (Fig. 6). Moreover, the work reported here extends recent findings (41), that KLRG1⁺ CD8⁺ T cell population is heterogeneous, as it contains both differentiated (EM28⁻) and less differentiated (EM28⁺) cells. Our observations further indicate that KLRG1 expression is associated to distinct TCR-BV clonotypes (Fig. 5), regardless of their differentiation status. Although KLRG1 is expressed on T

cells that have undergone a large number of cell divisions (43, 44), the function of this molecule has not been fully explored. Recently, Gründemann and coworkers (45) identified E-cadherin as a ligand for murine KLRG1, and proposed that its ligation by E-cadherin in healthy tissues may exert an inhibitory effect on primed T cells. In addition, mouse KLRG1 also binds to N- or R-cadherin (46), but ligand(s) for human KLRG1 have yet to be defined. Because in our tumor model, KLRG1 expression was preferentially observed on BV13-specific T cell clonotypes displaying increased *in vivo* cell turnover, another hypothesis is that KLRG1 downstream receptor signaling may be involved in promoting long-term survival of cells rather than their inhibition (47). Alternatively, KLRG1 expression is preferentially up-regulated in strongly proliferating clonotypes and may allow their specific inhibition by ligand-expressing tissues or melanoma cells.

Emerging findings suggest that the expression of PD-1 contributes to the functional impairment that characterizes T cells during chronic viral infections, because blocking the PD-1/PD-1L pathway enhances both proliferation and effector functions of "exhausted" T cells (48–51). Intriguingly, these results do not exactly support those obtained here in which chronically expanded tumor-reactive T cells expressing PD-1 also retained their capacity to undergo proliferation, cytokine production, and cytotoxic activity. Both BV8 and BV13 NY-ESO-1-specific T cell clonotypes efficiently secreted effector mediators such as granzyme B and perforin and killed tumor cells when tested directly *ex vivo* in a LiveCount assay (Fig. 4). Moreover, an important proportion of EM28⁻ NY-ESO-1-specific T cells were able to release IFN- γ upon stimulation with cognate peptide. Ongoing studies on blood samples from patient LAU 444, who exhibited a persisting and dominant Melan-A-specific CD8⁺ T cell response (13) further emphasized the finding that PD-1 was preferentially expressed within the differentiated EM28⁻ compartment, whereas IL-7R α expression was mostly found on EM28⁺ cells (data not shown). Collectively, our data strongly support the notion that circulating tumor-specific CD8⁺ T cell clonotypes not only share phenotypic features with that of differentiated cells but also exhibit functional characteristics similar to those of effective CTL specific for immunodominant viral Ags such as EBV or CMV (52). Whether PD-1 expression on tumor-reactive CTL may regulate such cells directly at the tumor site where melanoma cells, particularly in the presence of IFN- γ , express the PD-1L surface molecule (53), remains unclear and deserves additional studies.

We recently reported that both the natural T cell triggering by endogenous Ags and subsequent vaccination preferentially promoted an endogenous T cell clonotype with relatively high TCR avidity and antitumor activity (13). In the present study, we found that all individual T cell clonotypes that were identified after the start of immunotherapy were already present within the NY-ESO-1-specific CD8⁺ T cell response several months to years before vaccination. Importantly, both EM28⁺ and EM28⁻ compartments comprised the same T cell clonotypes, thus revealing a tight interplay of T cells in early and differentiated stages. These data suggest that effective therapeutic vaccination for cancer may only be accomplished in the presence of both memory (EM28⁺) and effector (EM28⁻) subsets of tumor-specific T cells and that multifactorial events determine the rise and fall of dominant clonotypes that contribute to dynamically sustain antitumor CD8⁺ T cell-mediated immunity.

Acknowledgments

We gratefully acknowledge patient LAU 50 for active participation, and the hospital staff for excellent collaboration. We gratefully thank

C. Barbey, J.-C. Cerottini, F. Lejeune, S. Leyvraz, D. Liénard, M. Matter, K. Muehlethaler, D. Rimoldi, and S. Salvi for collaboration and advice, I. Luescher and P. Guillaume for multimers, Seppic for Montanide ISA-51 (IFA). We also thank the excellent technical and secretarial help of C. Geldhof, R. Milesi, D. Mináidis, N. Montandon, and M. van Overloop.

Disclosures

The authors have no financial conflict of interest.

References

- Zinkernagel, R. M., and P. C. Doherty. 1997. The discovery of MHC restriction. *Immunol. Today* 18: 14–17.
- Altman, J. D., P. A. Moss, P. J. Goulder, D. H. Barouch, M. G. McHeyzer-Williams, J. I. Bell, A. J. McMichael, and M. M. Davis. 1996. Phenotypic analysis of antigen-specific T lymphocytes. *Science* 274: 94–96.
- Romero, P., P. R. Dunbar, D. Valmori, M. Pittet, G. S. Ogg, D. Rimoldi, J. L. Chen, D. Lienard, J. C. Cerottini, and V. Cerundolo. 1998. Ex vivo staining of metastatic lymph nodes by class I major histocompatibility complex tetramers reveals high numbers of antigen-experienced tumor-specific cytolytic T lymphocytes. *J. Exp. Med.* 188: 1641–1650.
- Butz, E. A., and M. J. Bevan. 1998. Massive expansion of antigen-specific CD8⁺ T cells during an acute virus infection. *Immunity* 8: 167–175.
- Moss, P. A., R. J. Moots, W. M. Rosenberg, S. J. Rowland-Jones, H. C. Bodmer, A. J. McMichael, and J. I. Bell. 1991. Extensive conservation of α and β chains of the human T-cell antigen receptor recognizing HLA-A2 and influenza A matrix peptide. *Proc. Natl. Acad. Sci. USA* 88: 8987–8990.
- Lehner, P. J., E. C. Wang, P. A. Moss, S. Williams, K. Platt, S. M. Friedman, J. I. Bell, and L. K. Borysiewicz. 1995. Human HLA-A0201-restricted cytotoxic T lymphocyte recognition of influenza A is dominated by T cells bearing the V β 17 gene segment. *J. Exp. Med.* 181: 79–91.
- Annels, N. E., M. F. Callan, L. Tan, and A. B. Rickinson. 2000. Changing patterns of dominant TCR usage with maturation of an EBV-specific cytotoxic T cell response. *J. Immunol.* 165: 4831–4841.
- Price, D. A., J. M. Brenchley, L. E. Ruff, M. R. Betts, B. J. Hill, M. Roederer, R. A. Koup, S. A. Migueles, E. Gostick, L. Wooldridge, et al. 2005. Avidity for antigen shapes clonal dominance in CD8⁺ T cell populations specific for persistent DNA viruses. *J. Exp. Med.* 202: 1349–1361.
- Trautmann, L., M. Rimbart, K. Echasserieau, X. Saulquin, B. Neveu, J. Dechanet, V. Cerundolo, and M. Bonneville. 2005. Selection of T cell clones expressing high-affinity public TCRs within human cytomegalovirus-specific CD8 T cell responses. *J. Immunol.* 175: 6123–6132.
- Pantaleo, G., J. F. Demarest, H. Soudeyns, C. Graziosi, F. Denis, J. W. Adelsberger, P. Borrow, M. S. Saag, G. M. Shaw, R. P. Sekaly, et al. 1994. Major expansion of CD8⁺ T cells with a predominant V β usage during the primary immune response to HIV. *Nature* 370: 463–467.
- Kalams, S. A., R. P. Johnson, A. K. Trocha, M. J. Dynan, H. S. Ngo, R. T. D'Aquila, J. T. Kurnick, and B. D. Walker. 1994. Longitudinal analysis of T cell receptor (TCR) gene usage by human immunodeficiency virus 1 envelope-specific cytotoxic T lymphocyte clones reveals a limited TCR repertoire. *J. Exp. Med.* 179: 1261–1271.
- Dong, T., G. Stewart-Jones, N. Chen, P. Easterbrook, X. Xu, L. Papagno, V. Appay, M. Weekes, C. Conlon, C. Spina, et al. 2004. HIV-specific cytotoxic T cells from long-term survivors select a unique T cell receptor. *J. Exp. Med.* 200: 1547–1557.
- Speiser, D. E., P. Baumgaertner, C. Barbey, V. Rubio-Godoy, A. Moulin, P. Corthesy, E. Devevre, P. Y. Dietrich, D. Rimoldi, D. Lienard, et al. 2006. A novel approach to characterize clonality and differentiation of human melanoma-specific T cell responses: spontaneous priming and efficient boosting by vaccination. *J. Immunol.* 177: 1338–1348.
- Boon, T., P. G. Coulie, B. J. Van den Eynde, and P. van der Bruggen. 2006. Human T cell responses against melanoma. *Annu. Rev. Immunol.* 24: 175–208.
- Silins, S. L., S. M. Cross, S. L. Elliott, S. J. Pye, S. R. Burrows, J. M. Burrows, D. J. Moss, V. P. Argat, and I. S. Misko. 1996. Development of Epstein-Barr virus-specific memory T cell receptor clonotypes in acute infectious mononucleosis. *J. Exp. Med.* 184: 1815–1824.
- Levitsky, V., P. O. de Campos-Lima, T. Frisan, and M. G. Masucci. 1998. The clonal composition of a peptide-specific oligoclonal CTL repertoire selected in response to persistent EBV infection is stable over time. *J. Immunol.* 161: 594–601.
- Posavad, C. M., M. L. Huang, S. Barcy, D. M. Koelle, and L. Corey. 2000. Long term persistence of herpes simplex virus-specific CD8⁺ CTL in persons with frequently recurring genital herpes. *J. Immunol.* 165: 1146–1152.
- Islam, S. A., C. M. Hay, K. E. Hartman, S. He, A. K. Shea, A. K. Trocha, M. J. Dynan, N. Reshamwala, S. P. Buchbinder, N. O. Basgoz, and S. A. Kalams. 2001. Persistence of human immunodeficiency virus type 1-specific cytotoxic T-lymphocyte clones in a subject with rapid disease progression. *J. Virol.* 75: 4907–4911.
- Meyer-Olson, D., K. W. Brady, M. T. Bartman, K. M. O'Sullivan, B. C. Simons, J. A. Conrad, C. B. Duncan, S. Lorey, A. Siddique, R. Draenert, et al. 2006. Fluctuations of functionally distinct CD8⁺ T-cell clonotypes demonstrate flexibility of the HIV-specific TCR repertoire. *Blood* 107: 2373–2383.
- Le Gal, F. A., V. M. Widmer, V. Dutoit, V. Rubio-Godoy, J. Schrenzel, P. R. Walker, P. J. Romero, D. Valmori, D. E. Speiser, and P. Y. Dietrich. 2007. Tissue homing and persistence of defined antigen-specific CD8⁺ tumor-reactive T-cell clones in long-term melanoma survivors. *J. Invest. Dermatol.* 127: 622–629.
- Baumgaertner, P., N. Rufer, E. Devevre, L. Derre, D. Rimoldi, C. Geldhof, V. Voelter, D. Lienard, P. Romero, and D. E. Speiser. 2006. Ex vivo detectable human CD8 T-cell responses to cancer-testis antigens. *Cancer Res.* 66: 1912–1916.
- Marcolino, I., G. K. Przybylski, M. Koschella, C. A. Schmidt, D. Voehringer, M. Schlesier, and H. Pircher. 2004. Frequent expression of the natural killer cell receptor KLRG1 in human cord blood T cells: correlation with replicative history. *Eur. J. Immunol.* 34: 2672–2680.
- Rufer, N., P. Reichenbach, and P. Romero. 2005. Methods for the ex vivo characterization of human CD8⁺ T subsets based on gene expression and replicative history analysis. *Methods Mol. Med.* 109: 265–284.
- Arden, B., S. P. Clark, D. Kabelitz, and T. W. Mak. 1995. Human T-cell receptor variable gene segment families. *Immunogenetics* 42: 455–500.
- Roux, E., C. Helg, F. Dumont-Girard, B. Chapuis, M. Jeannet, and E. Roosnek. 1996. Analysis of T-cell repopulation after allogeneic bone marrow transplantation: significant differences between recipients of T-cell depleted and unmanipulated grafts. *Blood* 87: 3984–3992.
- Rufer, N., A. Zippelius, P. Batard, M. J. Pittet, I. Kurth, P. Corthesy, J. C. Cerottini, S. Leyvraz, E. Roosnek, M. Nabholz, and P. Romero. 2003. Ex vivo characterization of human CD8⁺ T subsets with distinct replicative history and partial effector functions. *Blood* 102: 1779–1787.
- Rufer, N., W. Dragowska, G. Thornbury, E. Roosnek, and P. M. Lansdorp. 1998. Telomere length dynamics in human lymphocyte subpopulations measured by flow cytometry. *Nat. Biotechnol.* 16: 743–747.
- Rufer, N., T. H. Brummendorf, S. Kolvraa, C. Bischoff, K. Christensen, L. Wadsworth, M. Schulzer, and P. M. Lansdorp. 1999. Telomere fluorescence measurements in granulocytes and T lymphocyte subsets point to a high turnover of hematopoietic stem cells and memory T cells in early childhood. *J. Exp. Med.* 190: 157–167.
- Rufer, N., M. Migliaccio, J. Antonchuk, R. K. Humphries, E. Roosnek, and P. M. Lansdorp. 2001. Transfer of the human telomerase reverse transcriptase (TERT) gene into T lymphocytes results in extension of replicative potential. *Blood* 98: 597–603.
- Devevre, E., P. Romero, and Y. D. Mahnke. 2006. LiveCount assay: concomitant measurement of cytolytic activity and phenotypic characterisation of CD8⁺ T-cells by flow cytometry. *J. Immunol. Methods* 311: 31–46.
- Valmori, D., V. Dutoit, D. Lienard, D. Rimoldi, M. J. Pittet, P. Champagne, K. Ellefsen, U. Sahin, D. Speiser, F. Lejeune, J. C. Cerottini, and P. Romero. 2000. Naturally occurring human lymphocyte antigen-A2 restricted CD8⁺ T-cell response to the cancer testis antigen NY-ESO-1 in melanoma patients. *Cancer Res.* 60: 4499–4506.
- Stewart-Jones, G. B., A. J. McMichael, J. I. Bell, D. I. Stuart, and E. Y. Jones. 2003. A structural basis for immunodominant human T cell receptor recognition. *Nat. Immunol.* 4: 657–663.
- Appay, V., P. R. Dunbar, M. Callan, P. Klenerman, G. M. Gillespie, L. Papagno, G. S. Ogg, A. King, F. Lechner, C. A. Spina, et al. 2002. Memory CD8⁺ T cells vary in differentiation phenotype in different persistent virus infections. *Nat. Med.* 8: 379–385.
- Kaech, S. M., J. T. Tan, E. J. Wherry, B. T. Konieczny, C. D. Surh, and R. Ahmed. 2003. Selective expression of the interleukin 7 receptor identifies effector CD8 T cells that give rise to long-lived memory cells. *Nat. Immunol.* 4: 1191–1198.
- Bouneaud, C., Z. Garcia, P. Kourilsky, and C. Pannetier. 2005. Lineage relationships, homeostasis, and recall capacities of central- and effector-memory CD8 T cells in vivo. *J. Exp. Med.* 201: 579–590.
- Kedzierska, K., V. Venturi, K. Field, M. P. Davenport, S. J. Turner, and P. C. Doherty. 2006. Early establishment of diverse T cell receptor profiles for influenza-specific CD8⁺CD62L^{hi} memory T cells. *Proc. Natl. Acad. Sci. USA* 103: 9184–9189.
- Baron, V., C. Bouneaud, A. Cumano, A. Lim, T. P. Arstila, P. Kourilsky, L. Ferradini, and C. Pannetier. 2003. The repertoires of circulating human CD8⁺ central and effector memory T cell subsets are largely distinct. *Immunity* 18: 193–204.
- Le Gal, F. A., M. Ayyoub, V. Dutoit, V. Widmer, E. Jager, J. C. Cerottini, P. Y. Dietrich, and D. Valmori. 2005. Distinct structural TCR repertoires in naturally occurring versus vaccine-induced CD8⁺ T-cell responses to the tumor-specific antigen NY-ESO-1. *J. Immunother.* 28: 252–257.
- Pantaleo, G., H. Soudeyns, J. F. Demarest, M. Vaccarezza, C. Graziosi, S. Paolucci, M. Daucher, O. J. Cohen, F. Denis, W. E. Biddison, et al. 1997. Evidence for rapid disappearance of initially expanded HIV-specific CD8⁺ T cell clones during primary HIV infection. *Proc. Natl. Acad. Sci. USA* 94: 9848–9853.
- Cohen, G. B., S. A. Islam, M. S. Noble, C. Lau, C. Brander, M. A. Altfeld, E. S. Rosenberg, J. E. Schmitz, T. O. Cameron, and S. A. Kalams. 2002. Clonotype tracking of TCR repertoires during chronic virus infections. *Virology* 304: 474–484.
- Ibegbu, C. C., Y. X. Xu, W. Harris, D. Maggio, J. D. Miller, and A. P. Kourits. 2005. Expression of killer cell lectin-like receptor G1 on antigen-specific human CD8⁺ T lymphocytes during active, latent, and resolved infection and its relation with CD57. *J. Immunol.* 174: 6088–6094.
- Thimme, R., V. Appay, M. Koschella, E. Panther, E. Roth, A. D. Hislop, A. B. Rickinson, S. L. Rowland-Jones, H. E. Blum, and H. Pircher. 2005. Increased expression of the NK cell receptor KLRG1 by virus-specific CD8 T cells during persistent antigen stimulation. *J. Virol.* 79: 12112–12116.

43. Voehringer, D., C. Blaser, P. Brawand, D. H. Raulet, T. Hanke, and H. Pircher. 2001. Viral infections induce abundant numbers of senescent CD8 T cells. *J. Immunol.* 167: 4838–4843.
44. Voehringer, D., M. Koschella, and H. Pircher. 2002. Lack of proliferative capacity of human effector and memory T cells expressing killer cell lectinlike receptor G1 (KLRG1). *Blood* 100: 3698–3702.
45. Grundemann, C., M. Bauer, O. Schweier, N. von Oppen, U. Lassing, P. Saudan, K. F. Becker, K. Karp, T. Hanke, M. F. Bachmann, and H. Pircher. 2006. Cutting edge: identification of E-cadherin as a ligand for the murine killer cell lectin-like receptor G1. *J. Immunol.* 176: 1311–1315.
46. Ito, M., T. Maruyama, N. Saito, S. Koganei, K. Yamamoto, and N. Matsumoto. 2006. Killer cell lectin-like receptor G1 binds three members of the classical cadherin family to inhibit NK cell cytotoxicity. *J. Exp. Med.* 203: 289–295.
47. Ugolini, S., C. Arpin, N. Anfossi, T. Walzer, A. Cambiaggi, R. Forster, M. Lipp, R. E. Toes, C. J. Melief, J. Marvel, and E. Vivier. 2001. Involvement of inhibitory NKR1 in the survival of a subset of memory-phenotype CD8⁺ T cells. *Nat. Immunol.* 2: 430–435.
48. Barber, D. L., E. J. Wherry, D. Masopust, B. Zhu, J. P. Allison, A. H. Sharpe, G. J. Freeman, and R. Ahmed. 2006. Restoring function in exhausted CD8 T cells during chronic viral infection. *Nature* 439: 682–687.
49. Day, C. L., D. E. Kaufmann, P. Kiepiela, J. A. Brown, E. S. Moodley, S. Reddy, E. W. Mackey, J. D. Miller, A. J. Leslie, C. DePierres, et al. 2006. PD-1 expression on HIV-specific T cells is associated with T-cell exhaustion and disease progression. *Nature* 443: 350–354.
50. Trautmann, L., L. Janbazian, N. Chomont, E. A. Said, S. Gimmig, B. Bessette, M. R. Boulassel, E. Delwart, H. Sepulveda, R. S. Balderas, et al. 2006. Upregulation of PD-1 expression on HIV-specific CD8⁺ T cells leads to reversible immune dysfunction. *Nat. Med.* 12: 1198–1202.
51. Petrovas, C., J. P. Casazza, J. M. Brenchley, D. A. Price, E. Gostick, W. C. Adams, M. L. Prekopio, T. Schacker, M. Roederer, D. C. Douek, and R. A. Koup. 2006. PD-1 is a regulator of virus-specific CD8⁺ T cell survival in HIV infection. *J. Exp. Med.* 203: 2281–2292.
52. Appay, V., C. Jandus, V. Voelker, S. Reynard, S. E. Coupland, D. Rimoldi, D. Lienard, P. Guillaume, A. M. Krieg, J. C. Cerottini, et al. 2006. New generation vaccine induces effective melanoma-specific CD8⁺ T cells in the circulation but not in the tumor site. *J. Immunol.* 177: 1670–1678.
53. Dong, H., S. E. Strome, D. R. Salomao, H. Tamura, F. Hirano, D. B. Flies, P. C. Roche, J. Lu, G. Zhu, K. Tamada, et al. 2002. Tumor-associated B7-H1 promotes T-cell apoptosis: a potential mechanism of immune evasion. *Nat. Med.* 8: 793–800.